Memory and correlation effects in nuclear collisions

H. S. Köhler
Physics Department, University of Arizona, Tucson, Arizona 85721
(Received 16 December 1994)

Relaxation rates are calculated by numerically solving the Kadanoff-Baym equations for an extended system of nuclear matter. The time evolutions of initial nonequilibrium distributions in momentum space, defined by two Fermi spheres, is studied. Comparisons are made with the (semi-) classical method used in BUU, VUU, etc. Danielewicz has found that at a nucleon density of ~ 0.3 nucleon/fm^3 and an equilibrated temperature of about 70 MeV, the quantum relaxation rate is smaller than the classical by a factor of about 2. These results are confirmed. The calculations are extended to lower temperatures (energies) and densities and this ratio is found to be essentially unchanged over a wide range although there are deviations from this rule as seen in the text. The quantum evolutions are started either with an uncorrelated or a correlated initial distribution. The latter are obtained with imaginary time stepping. The relaxation time approximation was previously found to be excellent for the classical evolution. It is found to be as good for the quantum evolution. The memory time is in the present calculations found to be less than 5 fm/c (i.e., $\sim 1.7 \times 10^{-23}$ s). One concludes that quantum-mechanical effects have to be incorporated in the models of heavy ion collisions and nuclear dynamics. Not until this is done comprehensively will one be able to readily assess the role of two-nucleon collisions in the equilibration process.

PACS number(s): 25.70.−z, 05.20.Dd, 05.60.+w, 21.65.+f

I. INTRODUCTION

The transport models mostly used in the analysis of nuclear collisions are based upon the Nordheim-Uehling-Uhlenbeck extension of the Boltzmann equation to include the Fermi-Dirac blocking in the collision term [1,2]. Including also the scatterings by the Vlasov mean field yields the semiclassical BUU, VUU, Landau-Vlasov, etc., models. These provide a good basis for understanding a variety of effects seen in nuclear collisions such as energy dissipation, collective transverse flow, etc. The extraction of quantitative results from these classical quasiparticle models applied to collisions in the dense nuclear medium has however been questioned repeatedly.

In previously published work collision rates were calculated using the classical collision term in homogeneous nuclear matter. The result was expressed in terms of a density and temperature dependent relaxation time [3]. In the present report quantum-mechanical corrections are included in the calculation of relaxation times.

One quantum-mechanical correction discussed repeatedly is replacing the free cross section (or T matrix) in the collision term with a medium corrected effective interaction [4–8]. Other corrections involves also including the energy dependence, i.e., the time delay of these interactions, which has not yet been done.

Another correction stems from the situation that in the nonequilibrium systems formed in nuclear collisions the single-particle states have finite lifetimes. The widths of these states are not included in the classical treatment where the individual NN collisions conserve energy. Furthermore, all interactions are pointlike in time and retardation effects are neglected.

All these effects are contained in the quantum-mechanical treatment of the dynamics of many-body systems by Kadanoff and Baym [9], with a simultaneous use of a many-body effective interaction such as the Brueckner K matrix (but preferably with hole-hole propagator included). The Kadanoff-Baym (KB) equations describe the system in terms of one-body Green's functions. In the quasiparticle approximation and neglecting memory effects they reduce to the Markovian dynamics in a Boltzmann-like classical transport equation. In this latter case individual nucleon-nucleon scatterings conserve energy while those allowing for the finite width of the states in the correlated medium are neglected. A related effect is that all interactions are pointlike in time while the memory effect which is contained in the Kadanoff-Baym equations are neglected.

There are several studies of memory and correlation effects based on approximate solutions of the KB equations, e.g., Refs. [10–13]. In this paper are shown some "exact" numerical results of calculations with these equations. It will be the subject of a future investigation to do comparisons with the approximate solutions and thus obtain further insight into the quantal corrections.

A numerical study of a quantum theoretical time-dependent density-matrix theory (TDDM) that includes a collision term was done by Tohyama in two-dimensional geometry [14].

Other noteworthy work somewhat related to the present includes works by Ko *et al.* [15].

Danielewicz solved the Kadanoff-Baym equations numerically for nuclear matter [16]. He calculated the relaxation of a system consisting of two Fermi spheres separated by a momentum corresponding to an equilibrated temperature of 70 MeV and a total density of ~ 0.3 nucleon/fm^3. His detailed investigation revealed that the quantum evolution has an equilibration time almost twice

as large as that of the classical. We confirm this result and the comparison is extended to lower energies and densities.

The KB equations and the classical limit are shortly reviewed in Secs. II and III. Some computational details are shown in Sec. IV and the results of the numerical study is then given in Sec. V. Section VI contains a summary and comments.

II. QUANTUM EVOLUTION

Only a short presentation of the relevant equations is given here. Detailed derivations are found in the book by Kadanoff and Baym [9] and in [17–19]. In homogeneous nuclear matter and neglecting the mean field the KB equations reduce to

$$\left(i\hbar\frac{\partial}{\partial t}+\frac{p^2}{2m}\right)G^{\gtrless}(\mathbf{p},t,t') = \int_{t_0}^{t} dt''[\Sigma^{>}(\mathbf{p},t,t'')-\Sigma^{<}(\mathbf{p},t,t'')]G^{\gtrless}(\mathbf{p},t'',t') - \int_{t_0}^{t'} dt''\,\Sigma^{\gtrless}(\mathbf{p},t,t'')[G^{>}(\mathbf{p},t'',t')-G^{<}(\mathbf{p},t'',t')]. \tag{2.1}$$

The notations are conventional; $G^{>}$ and $G^{<}$ are essentially the occupation numbers for hole and particles, respectively. Specifically the distribution function $f(\mathbf{p},t)$ is given by

$$f(\mathbf{p},t) = -iG^{<}(\mathbf{p},t,t)\ . \tag{2.2}$$

The scattering rates Σ are given by

$$\Sigma^{\gtrless}(\mathbf{p},t,t') = -i\hbar\int\frac{d^3\mathbf{p_1}}{(2\pi)^3}\left\langle\tfrac{1}{2}(\mathbf{p}-\mathbf{p_1})\mid T^{\gtrless}(\mathbf{p}+\mathbf{p_1},t,t')\mid\tfrac{1}{2}(\mathbf{p}-\mathbf{p_1})\right\rangle G^{\lessgtr}(\mathbf{p_1},t',t)\ . \tag{2.3}$$

Here $T^{\gtrless}$ is defined by

$$\left\langle\mathbf{p}\mid T^{\gtrless}(\mathbf{P},t,t')\mid\mathbf{p}\right\rangle = \int dt''dt'''d\mathbf{p}''d\mathbf{p}'''\left\langle\mathbf{p}\mid T^{+}(\mathbf{P},t,t'')\mid\tfrac{1}{2}(\mathbf{p}''-\mathbf{p}''')\right\rangle \times G^{\gtrless}(\mathbf{p}'',t'')G^{\gtrless}(\mathbf{p}''',t''')\left\langle\tfrac{1}{2}(\mathbf{p}''-\mathbf{p}''')\mid T^{-}(\mathbf{P},t,t'')\mid\mathbf{p}\right\rangle\ . \tag{2.4}$$

The effective interaction $T^{\pm}$ (essentially the Brueckner K matrix but with hole-hole ladders) is defined in terms of an integral equation formally written as

$$T_{12}^{\pm} = V + VG_1^{\pm}G_2^{\pm}T_{12}^{\pm}\ , \tag{2.5}$$

where V is the "free" N-N interaction potential.

III. CLASSICAL EVOLUTION

The classical limit of the Kadanoff-Baym equations has been discussed repeatedly in the literature [9,17,19]. This is often done using the KB ansatz

$$G^{<}(\mathbf{p},T,\tau) = if(p,T)a(\mathbf{p},T,\tau), \tag{3.1}$$

$$G^{>}(\mathbf{p},T,\tau) = -i[1-f(\mathbf{p},T)]a(\mathbf{p},T,\tau)\ , \tag{3.2}$$

where $T=(t+t')/2$ and $\tau=t-t'$ and a is the spectral function defined by

$$a(\mathbf{p},T,\tau) = i[G^{>}(\mathbf{p},T,\tau)-G^{<}(\mathbf{p},T,\tau)]\ . \tag{3.3}$$

This ansatz leads however to inconsistencies in time arguments of the memory effect. The discrepancy with other approaches was discussed by Jauho and Wilkins [20]. A generalized GKB ansatz was introduced by Lipavsky *et al.* [21,13] differing from the KB in the time argument of the distribution function. Following this work we use the ansatz

$$G^{<}(\mathbf{p},T,\tau) = if\left(\mathbf{p},T-\frac{\mid\tau\mid}{2}\right)a(\mathbf{p},T,\tau), \tag{3.4}$$

$$G^{>}(\mathbf{p},T,\tau) = -i\left[1-f\left(\mathbf{p},T-\frac{\mid\tau\mid}{2}\right)\right]a(\mathbf{p},T,\tau). \tag{3.5}$$

The spectral function can be written as

$$a(\tau) = e^{-1/2\Gamma\tau}e^{i\omega\tau}, \tag{3.6}$$

where Γ is the width of the particle state and ω its energy. Neglecting the mean field as done in the present calculations $\omega=p^2/2m$. In the limit of zero width, i.e., the quasiparticle limit, the time integration in Eq. (2.1) reduces to

$$\int d\tau\,\cos[(\omega+\omega_1-\omega'-\omega_1')\tau/\hbar][FF_1f'f_1'-ff_1F'F_1'], \tag{3.7}$$

with $f\equiv f(\mathbf{p},t-\tau)$ and $F\equiv 1-f$, etc. With the KB ansatz the time argument would have been $t-\tau/2$ instead of $t-\tau$. The memory effect involves an integration over *past* distribution functions. This effect is evidently important if the relaxation time is short compared to the memory time itself and its importance has been demonstrated in several calculations [10–13]. If neglecting the effect, i.e., with $f\equiv f(\mathbf{p},t)$ and $F\equiv 1-f$, etc., the time integration reduces to a δ function over energies, i.e., the energy is conserved in each binary collision.

The result is in our case the Boltzmann equation

with the Nordheim-Uehling-Uhlenbeck modification for fermions.

For the case of the local interaction used here [Eq. (4.1)] this classical equation is given by [16]

$$\frac{\partial f(\mathbf{p},t)}{\partial t} = 4\int \frac{d\mathbf{p_1}}{(2\pi)^3} d\Omega'(\mid \mathbf{p}-\mathbf{p}' \mid /m)(m^2/16\pi^2) \times \mid V(\mathbf{p}'-\mathbf{p}) \mid^2 [FF_1f'f_1' - ff_1F'F_1'] , \tag{3.8}$$

where $f \equiv f(\mathbf{p},t)$ and $F \equiv 1-f$, etc.

IV. COMPUTATIONAL DETAILS

To make the calculations reasonably short and to allow for direct comparison with Ref. [16] the effective interaction $T^{\pm}$ [defined by Eq. (2.5)] is here approximated by the simple Gaussian form potential used by Danielewicz [16] and defined by

$$V(\mathbf{p}) = \pi^{3/2}\eta^3 V_0 e^{-\frac{1}{4}\eta^2 p^2} . \tag{4.1}$$

For the Green's function scattering rates in Eq. (2.3) one then obtains [16]

$$\Sigma^{>}_{<}(\mathbf{p},t,t') = 4\hbar \int \frac{d^3\mathbf{p_1}}{(2\pi)^3}\int \frac{d^3\mathbf{p}'}{(2\pi)^3} \mid V(\mathbf{p}'-\mathbf{p}) \mid^2 \times G^{>}_{<}(\mathbf{p}',t,t') G^{>}_{<}(\mathbf{p}+\mathbf{p_1}-\mathbf{p}',t,t') \times G^{<}_{>}(\mathbf{p_1},t',t) . \tag{4.2}$$

The same parameters are used for η and V_0 as used by Danielewicz [16]. Thus $\eta = 0.57$ fm and $V_0 = -453$ MeV.

The quantum evolution equations are solved for various initial (uncorrelated) distributions $f(\mathbf{p},0)$ that define $G^{<}(\mathbf{p},0,0)$ by Eq. (2.2) and $G^{>}(\mathbf{p},0,0) = -i + G^{<}(\mathbf{p},0,0)$. In spite of the apparent complexity, the calculations with the KB equations are relatively simple in comparison with the corresponding classical limit, i.e., Eq. (3.8). The simplicity is however restricted to the choice of a local potential as in Eq. (4.1). In this case the convolution theorem for Fourier transforms speeds up the evaluation of the integrations in Eq. (4.2) enormously.

In addition to doing calculations with initially uncorrelated distributions, they were also made with initially correlated distributions obtained by imaginary time stepping as described in detail by Danielewicz [17,16]. This implies first preparing an initially correlated system by repeated imaginary time stepping along positive and negative axes iterating to self-consistency. The time stepping is then extended to the real axes as well.

The numerical work was in essence performed as in Ref. [16], but the computer program was developed independently. As noted above the scattering rates in Eq. (4.2) were calculated by means of Fourier transforms. Danielewicz used a cylindrical coordinate system while Cartesian coordinates were used here although all results reported here are for cylindrically symmetric systems.

The system was contained in a box of size $8\times4\times4$ fm^{-1} in momentum space with a mesh $\delta p = 0.2$ or 0.15. The time stepping was made in a predictor corrector method with a time mesh $\delta t = 0.5$ fm/c. Much computing time was used to ascertain that these meshes were adequate. The time differential ∂G (or ∂f) at time t was calculated from the average of the derivative at time t and time $t+\delta t$, with the derivative at time $t+\delta t$ calculated from a first iteration. The evolution was in general studied for 20 time steps. The integration along the imaginary axes was in general done for ± 3 fm/c.

In the cases of the correlated initial distributions the correlated Green's functions were obtained in a 15-step iterative calculation.

In the quantum evolution the number of particles was in general conserved to within 0.2% and the energy to less than 1% over the 20 time steps usually used.

In the Boltzmann case the calculations were made as in the previously published report [3]. The integrations were made on a mesh either with trapezoidal or Gaussian weights. The particle and energy conservation was sometimes less accurate in this case being more sensitive to the sharp cutoff of the zero-temperature Fermi spheres.

V. RESULTS OF CALCULATIONS

A. Zero temperature calculation

If the classical equation (3.8) is time evolved starting with a Fermi distribution it will be stationary, because this is a solution of $\partial f/\partial t = 0$. This is not the case for the quantum evolution. In the latter case it is the Green's functions for the correlated system that is stationary. An initially uncorrelated distribution time evolves with a build-up of correlations and after about 5 fm/c one finds a stationary distribution function that differs from the initial Fermi distribution. This is exemplified by Fig. 1 in a calculation starting with a T=0 Fermi distribution at a density of 0.185 nucleon/fm^3. The step function in the figure is the uncorrelated distribution function at temperature $T = 0$ while the second curve shows the stationary

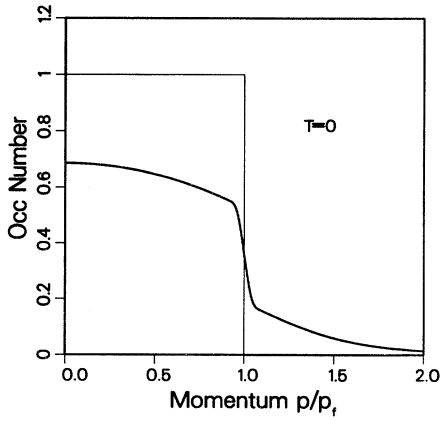

FIG. 1. The solid lines show the distribution function $f(\mathbf{p}, t = 5$ fm/$c)$ at normal density. $f(\mathbf{p}, t = 0)$ was an uncorrelated Fermi distribution of temperature $T = 0$ and is shown by the step function.

distribution obtained after correlations have developed at 5 fm/c. The occupation numbers at the bottom of the Fermi sea are seen to be depleted to about 0.7.

The time evolution of this calculation is illustrated by Fig. 2. The potential energy, shown by the lowest curve is seen to initially decrease until the correlations are built up. As the potential energy decreases during the first 3–4 fm/c, the kinetic energy shown by the upper curve increases, while the total energy shown by the middle curve is seen to be constant at about 24.5 MeV, which is of course also the kinetic energy of the initial uncorrelated Fermi distribution, because the KB equations conserve total energy (as well as particle number).

Although the initial uncorrelated system is at $T = 0$, i.e., in its ground state the final correlated state is not. During the build-up of correlations the total energy is conserved by Eq. (2.1), while the ground state of the correlated system should have a lower energy because of the binding. Therefore the temperature is actually larger than zero even though in the presentation of results of the calculations they are always labeled by the temperature of the initial uncorrelated system (see Sec. V C) although the actual temperature of the correlated system then is larger. The ground state for the correlated system is obtained by the method of imaginary time stepping referred to in Sec. IV. The occupation numbers obtained in this case are shown in Fig. 3, from which one finds a depletion to about 0.90, i.e., appreciably less depletion than in Fig. 1. For comparison, Brueckner calculations with realistic interactions gives a depletion to about 0.82 [22]. The total energy is reduced relative to the uncorrelated case by about 8 MeV/nucleon with a potential energy of −19 MeV/nucleon and a kinetic energy of 32 MeV/nucleon to be compared with −22 MeV/nucleon and 48 MeV/nucleon, respectively, in the uncorrelated case.

The spectral function a and the width Γ is readily calculated from Eqs. (3.3) and (3.6). A width of $\sim$ 32 MeV (almost independent of momentum) is obtained in the present case for the correlated system. This agrees qualitatively with Brueckner [23] and other theories in calculations with realistic forces. In the present calculations the width is however not zero at the Fermi surface as would be anticipated. In the uncorrelated system, i.e., at the onset of the time evolution the width is of course zero for all momenta.

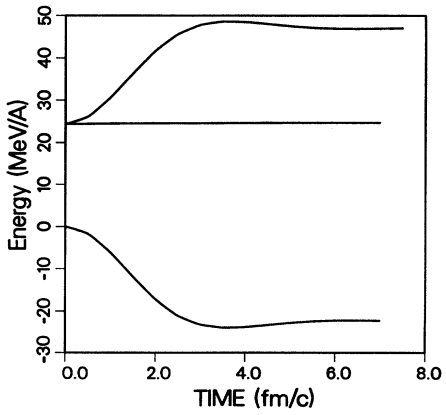

FIG. 2. The kinetic, total, and potential energies per nucleon is shown by the top, middle, and bottom curves as a function of time as the correlations build up in an initially uncorrelated nuclear matter of zero temperature and a density of 0.185 nucleon/fm^3.

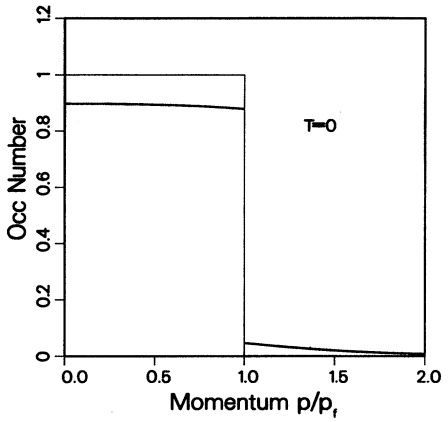

FIG. 3. Similar to Fig. 1 but with imaginary time stepping. Note that the depletion of occupations in the Fermi sea is now reduced because of a lower temperature.

B. Quasi-particle limit

The correlation effects should decrease as the quasi-particle limit is reached at low density and high temperature. Figure 4 shows the thermalization of an initial distribution of two Fermi spheres with the temperature 10 MeV and chemical potential −12 MeV separated by 2.5 fm^{-1}. The equilibrated temperature is then 33 MeV.

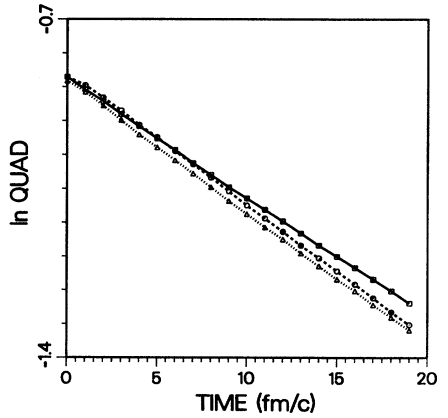

FIG. 4. The logarithm of the quadrupole moment of the distribution in momentum space as a function of time. The solid line is for the classical case, the broken line for the quantum case with an uncorrelated initial distribution, while the dotted line is for an initially correlated system. This figure illustrates the near agreement between the three cases. The temperature as defined in the text is here 33 MeV and the density is 1/10 of normal nuclear matter.

The classical distribution (solid line) equilibrates with $\tau_{\rm rel}$=39 fm/c. In the quantum cases the relaxation is initially smaller but reaches a value of $\tau_{\rm rel}$=36 fm/c after about 5 fm/c. As discussed in Sec. III one has to neglect not only the correlations but also the memory effect to recover the classical equation, Eq. (3.8). Numerically this requires however an integration over a sufficiently long time that the δ function over energies in the Boltzmann equation is recovered. This may explain the delay in establishing a constant relaxation time in the quantum case. The difference in relaxation times is numerically acceptable. One has to bear in mind that the two computer programs are widely different. Although the system is *a priori* expected to be quasiparticle there is still a binding energy of $\sim$ 4 MeV and the actual temperature of the quantum distributions is slightly higher than that of the classical which also may explain why the quantum relaxation time is somewhat smaller. It should be noted that the reverse is seen in the results of higher density that are shown below. Which is the most important difference in the present case, memory or width, is unknown.

C. Relaxation rates

To study the equilibrations and compare the quantum and classical cases the time evolution was in general started with a distribution consisting of two Fermi spheres at zero temperature separated by some momentum. Two separate calculations are made in the quantum case. In the first the time evolution is started with the initially uncorrelated state. In the second the system was first time evolved by imaginary time stepping as described in Sec. IV.

For the presentation of the results, the total density ρ and the temperature T of the final equilibrated distribution serves as parameters. The temperature was obtained from the kinetic energy and density of the initially *uncorrelated* system of the two spheres by inverting the well-known expression for the kinetic energy as a function of temperature for an equilibrated Fermi distribution. In previous work it was in fact found that this parametrization is very useful. To a very good approximation the relaxation rate is found to be the same for different distributions in momentum space if only the *final* temperature and density is the same [3]. This ansatz was also used by Bertsch in his expression for the relaxation of a quadrupole deformation [25].

Because of the correlations some caution in interpreting the results is however necessary with this definition of the temperature as will be discussed below.

When time evolving the initially uncorrelated system the correlations are building up during the first 3–5 fm/c with changes in potential and kinetic energy as shown in Fig. 2. In the correlated case these energies are practically constant during the evolution along the real time axis.

In several previous publications the author has used the relaxation time method to include the NN collisions in extended TDHF calculations for heavy ion collisions [24]. This involves calculating the collision term by

$$\left(\frac{\partial\rho(\mathbf{r},\mathbf{r}',t)}{\partial t}\right)_{\rm coll} = -\frac{\rho(\mathbf{r},\mathbf{r}',t)-\rho_{\mathbf{0}}(\mathbf{r},\mathbf{r}',t)}{\tau_{\rm rel}[T(\mathbf{r},t),\rho(\mathbf{r},\mathbf{r},t)]}, \qquad (5.1)$$

where $\rho(\mathbf{r},\mathbf{r}')$ is the density matrix and $\rho_{\mathbf{0}}$ is the local equilibrated density matrix, i.e., (in Wigner space) a Fermi distribution with a local temperature $T(\mathbf{r})$. $\rho(\mathbf{r},\mathbf{r})$ is the nucleon density.

The relaxation time method relies on the exponential decay of the distribution. More precisely, one expects each multipole of the distribution in momentum space to have a separate relaxation time. In a previous publication relaxation times were calculated in the classical case for the quadrupole and other deformations and the exponential decay law was verified to a high degree of accuracy in all cases [3]. Figure 5 shows that this also holds very well for the quantum case, after a memory time of a few fm/c has been reached. Before this initial time the relaxation is slower. The figure shows only the relaxation time for the quadrupole moment, and this relates to the viscosity of the system which of course is very important for the dynamics. While the moments decay exponentially in agreement with that, Eq. (5.1) is a good approximation this does not hold true for the anisotropy parameter $q = 2\frac{\langle p_z^2\rangle}{\langle p_x^2\rangle+\langle p_y^2\rangle} - 1$ used in Ref. [16]. The result of the relaxation-rate calculations can because of the constancy of $\tau_{\rm rel}$ during the equilibration be summarized by the widths $\hbar/\tau_{\rm rel}$, and these are plotted as a function of temperature at three densities as shown in Figs. 6–8. The solid line in each of these figures shows the classical widths as a function of temperature at three densities corresponding roughly to normal, half, and double nuclear matter density. Note that the vertical scales are different for each density. In each case the classical width is seen to go to zero with the temperature. This is in agreement with the well-known behavior for any fermion system. It increases sharply as a function of density and also with temperature until reaching a maximum after which it decreases somewhat. This is in general agreement with previous calculations of relaxation times [3]. The dotted and broken curves in Figs. 6, 7, and 8 are for the quantum

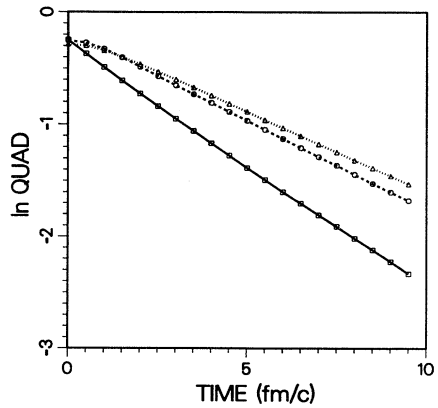

FIG. 5. Similar to Fig. 4 except that the final temperature now is 45 MeV and the density is that of normal nuclear matter. Note the difference in vertical scale.

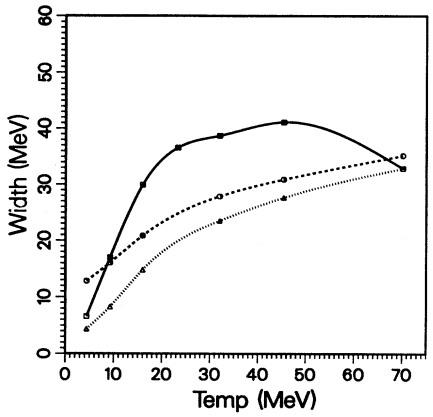

FIG. 6. The width, i.e., $\hbar/\tau_{\rm rel}$, as a function of the temperature of the equilibrated system. The curves are labeled as in Fig. 4. The total density is here that for normal nuclear matter.

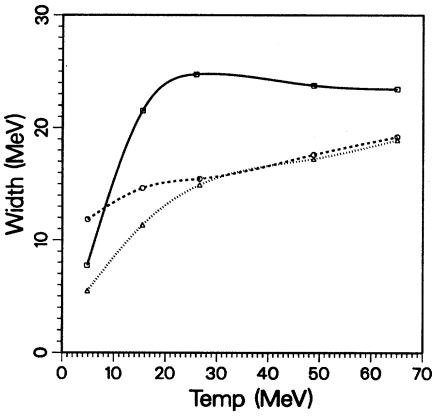

FIG. 7. Same as Fig. 6 except that the density is half nuclear matter density. Note the difference in vertical scale.

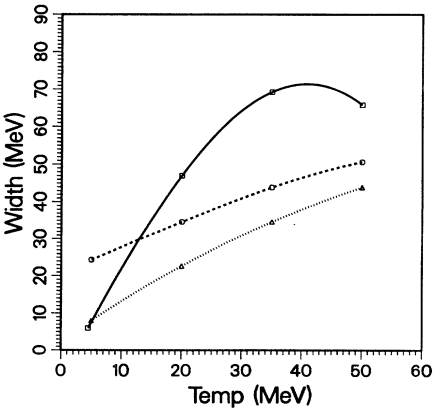

FIG. 8. Same as Fig. 6 except that the density is double nuclear matter density. Note the difference in vertical scale.

cases with and without an initially correlated state with the latter showing the smallest widths.

One observes that in general the widths are smaller, i.e., the relaxation times are longer in the quantum cases. At the higher density shown in Fig. 8 the ratio for the two cases is as large as two at 35 MeV. The width for an initially correlated state is smaller than for the corresponding uncorrelated. For the half normal density calculations the difference is especially large for temperatures below 20 MeV.

By extrapolating the widths for the initially uncorrelated systems one may be lead to the conclusion that there is a finite width of about 10 MeV even at zero temperature. This would be an interesting result with wide implications for nuclear dynamics. It was already discussed in Sec. V A that, although the initial system is uncorrelated, the correlations are already developed at about 5 fm/c (see Fig. 2) with the system simultaneously being excited. As a consequence the uncorrelated curves should really be shifted to higher temperatures. The importance of starting the time evolutions with correlations already built in are thus seen to be important for obtaining meaningful results. It is however interesting to see that even then the results indicate a nonzero width in the limit of zero temperature.

D. Memory time

In all the results presented so far in this paper the time integration in Eq. (2.1) is from time zero to the present time. Because the system has a finite memory it is however only necessary to start the integration from not more than about 5 fm/c back. This is illustrated by Fig. 9 showing the relaxation at a temperature of 45 MeV for four different memory times ranging from 1 to 5 fm/c. These are for an initially uncorrelated system. The curve for 5 fm/c (solid curve) coincides with the broken curve in Fig. 5 in which the time integration starts at time zero. It is seen that a memory time of only 1.5 fm/c

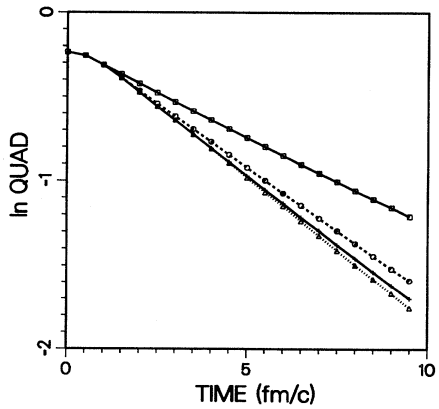

FIG. 9. This is similar to the broken curve in Fig. 5 except that four different memory times (see text) are used in the calculation. From top to bottom these are 1.0, 1.5, 5.0, and 2.0 fm/c, respectively.

would give a small error in relaxation time. Note that with the time mesh of $\delta t = 0.5$ fm/c that is used in the calculation this implies summing over only three points in the numerical integration in this case. A memory time of 5 fm/c agrees with Fig. 2 showing that an initially uncorrelated system is stationary after about that time (or less).

It should be noted that in an uncorrelated medium for which the width is zero the memory time is infinite. The time integration in Eq. (2.1) then starts (in principle) from $t = -\infty$ rather than from $t = 0$. This then leads to a δ function of the energy, i.e., energy is conserved in the two-body collisions as in the Boltzmann equation.

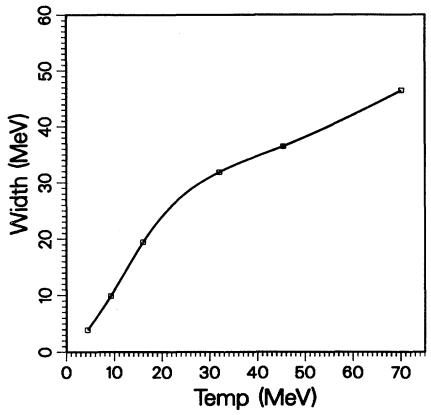

FIG. 10. Classical relaxation rates (widths) at normal density with a momentum-dependent interaction fitting the experimental free N-N cross sections. This should be compared with the upper curve in Fig. 6 which is for the momentum-independent interaction used in the present work [Eq. (4.1)].

VI. SUMMARY AND FINAL COMMENTS

This work confirms Danielewicz conclusions [16] that a quantum-mechanical treatment of the collision term in nuclear collisions is essential. The computer program used here was developed independently of his even though the general methods were the same especially as regards the use of Fourier transforms to compute the collision rates. The present calculations were however made in a three-dimensional Cartesian geometry instead of a cylindrical. The predictor corrector method used in the time stepping was the same in the two calculations. The present calculations agree numerically with his (to the extent that a comparison can be made).

The present calculations of the KB equations were relatively simple to perform, in fact simpler and computationally more accurate than the comparable classical calculations. So, for example, are the particle and energy conservations better satisfied. The simplicity is restricted to the use of a simple and not so realistic effective interaction and therefore the results can perhaps therefore not be taken as altogether general. The interaction used here [defined by Eq. (4.1)] depends only on momentum transfer while the more general interaction $T^{\pm}$ will depend also on relative momentum as well as on times t and t'. (In the Fourier transformed time representation on energy ω and total time T.) It would be desirable to include these effects as well, even though this would require appreciably more computer efforts. A somewhat related question regards the relation between the correlations included by the T-matrix approximation for the effective interaction and the correlations built up by the KB collision term. The width found in Sec. V A, in the zero-temperature limit and the width found from Brueckner calculations (with realistic forces), are numerically similar but the formal relationship between them is not established.

The momentum dependence of the effective interaction would certainly have to be included for a reliable estimate of the quantum relaxation times. Figure 10 shows the classical result with experimental energy-dependent cross sections at normal density showing as much as 30% smaller relaxation times. Using in-medium cross sections [4–8] would decrease these even further. The quantum corrections relative the classical are however expected to be similar for both types of interactions.

The mean field has been omitted in the propagations between scatterings in all the calculations presented here. The correction is essentially the effective mass. The relaxation rates should therefore be further reduced by a factor m^* which is ~ 0.8 for normal nuclear matter density.

It is anticipated that these "exact" calculations of the KB equations will make it possible to numerically test the various approximate treatments of these equations. In this paper the test was made of the purely classical (quasiparticle) limit used in BUU, etc. Other approximations are suggested by several researchers with particular emphasis on retardation effects, etc., with applications not only for nuclear collisions but also in solid state. The tests of such approximations will be reserved for future publications. They are expected to shed some light on the applicability and feasibility of these various suggestions.

ACKNOWLEDGMENTS

It is a pleasure to thank Professor Pawel Danielewicz for numerous helpful discussions, especially regarding computing methods during the course of this work. This work was supported in part by the National Science Foundation Grant No. PHY-9407146.

[1] L.W. Nordheim, Proc. Roy. Soc. **A119**, 689 (1928).
[2] E.A. Uehling and G.E. Uhlenbeck, Phys. Rev. C **43**, 552 (1993).
[3] M.M. Abu-Samreh and H.S. Köhler, Nucl. Phys. **A552**, 101 (1993).
[4] P. Grangé, J. Cugnon, and A. Lejeune, Nucl. Phys. **A373**, 365 (1987).
[5] T. Alm, G. Roepke, W. Bauer, F. Daffin, and M. Schmidt, submitted to Nucl. Phys.
[6] J. Dabrowski and H.S. Köhler, Nucl. Phys. **A489**, 303 (1989).
[7] B. ter Haar and R. Malfliet, Phys. Rep. **149**, 207 (1987).
[8] H.S. Köhler, Nucl. Phys. **A529**, 209 (1991).
[9] L.P. Kadanoff and G. Baym, *Quantum Statistical Mechanics* (Benjamin, New York, 1962).
[10] C. Greiner, K. Wagner, and P.-G. Reinhard, Phys. Rev. C **49**, 1693 (1994).
[11] S. Ayik and M. Dworzecka, Nucl. Phys. **A440**, 424 (1985); S. Ayik and J. Randrup, Phys. Rev. C **50**, 2947 (1994).
[12] K. Morawetz, R. Walke, and G. Roepke, Phys. Lett. A **190**, 96 (1994).
[13] K. Morawetz and G. Roepke, Phys. Rev. E **51**, 4246 (1995).
[14] M. Tohyama, Nucl. Phys. **A563**, 494 (1993).
[15] C.M. Ko, D. Agassi, and H.A. Weidenmüller, Ann. Phys. (N.Y.) **117**, 237 (1979).
[16] P. Danielewicz, Ann. Phys. (N.Y.) **152**, 305 (1984).
[17] P. Danielewicz, Ann. Phys. (N.Y.) **152**, 239 (1984).
[18] W.D. Kraeft, D. Kremp, W. Ebeling, and G. Röpke, *Quantum Statistics of Charged Particle Systems* (Akademie-Verlag, Berlin, 1986); D. Kremp, W.D. Kraeft, and A.J.D. Lambert, Physica **127A**, 72 (1984).
[19] Wim Botermans and Rudi Malfliet, Phys. Rep. **198**, 115 (1990).
[20] A.P. Jauho and J.W. Wilkins, Phys. Rev. B **29**, 1919 (1984).
[21] P. Lipavsky, V. Spicka, and B. Velicky, Phys. Rev. B **34**, 6933 (1986).
[22] H.S. Köhler, Nucl. Phys. **A537**, 64 (1992).
[23] H.S. Köhler, Phys. Rev. C **46**, 1687 (1992).
[24] H.S. Köhler, Nucl. Phys. **A494**, 281 (1989) (and references therein).
[25] G. Bertsch, Z. Phys. A **289**, 103 (1978).